A R C H I V E S O F M E T A L L U R G Y A N D M A T E R I A L S
Volume 60 2015 Issue 4
DOI: 10.1515/amm-2015-0449

J. MICHALCZYK*,#, K. WOJSYK**

DEVELOPMENT AND MODELLING OF THE METHOD OF MANDRELLESS SMALL-RADIUS TUBE BENDING

OPRACOWANIE I MODELOWANIE SPOSOBU BEZTRZPIENIOWEGO GIĘCIA RUR NA MAŁYCH PROMIENIACH

The paper reports the results of research aimed at creating theoretical grounds for a new method of mandrelless small-radius tube bending ($1.5D_r<R_g<2.5D_r$, where D_r – tube diameter, R_g – bending radius). As the result of applying such a methodology it is possible to carry out the bending process (with an angle of up to 180°) and obtain an ovalization and wall thinning in the bending area, which are much smaller than those in currently manufactured products. The currently used bending methods and bending equipment are able to achieve a minimum bending radius not less than three times the tube outer diameter. The research hypothesis has assumed the existence of tube bending methods that are more efficient that those known so far. Than methods do not rely on circular bending contours, but instead they may use other shaping die contours which has not been explored yet. Circular benders used in practice fail in that they do not yield the expected results on small radii and do not control the material flow (do not ensure its correct behaviour) in the bending zone. The literature review has shown that there are currently no theoretical studies, numerical analyses and experimental verifications related to the processes of mandrelless tube bending on small radii, i.e. for $1.5D \leq R \geq 2.5D$, where: (R - bending radius, D - tube outer diameter) up to an angle of 180°. Due to the lack of studies on this subject, in their approach to the numerical modelling of the problem, the authors of the paper were guided by their own experience in this field and made every effort to make the numerical model reflect the actual process as accurately as possible. They were only aided by the general knowledge accumulated in the literature on numerical modelling. To sum up, the purpose of the publication is to demonstrate that the change in the die recess towards a shape resembling an ellipse results in a change in the characteristics of metal flow (movement) along the tube perimeter and in a change in the stress characteristics and, as a consequence, a change in the tube cross-section in the bending zone. The research discussed in this paper seeks to establish the correct flow of material in the tube cross-section in the bending zone by determining the most efficient bender recess shape and friction surface forming, which will eliminate the excessive ovalization and upper wall thinning. The expected effect of implementing this bending technology will be increasing the flow capacity in energy systems, which will directly translate into a reduction of atmospheric CO emissions due to the lower energy consumption. In addition, the paper has presented the concepts of tools intended for the experimental verification of tube bending process.

Keywords: mandrelless tube bending, small bending radii

W pracy przedstawiono wyniki badań polegających na stworzeniu podbudowy teoretycznej do nowej metody beztrzpieniowego gięcia rur na małych promieniach ($1.5D_r<R_g<2.5D_r$,, gdzie D_r – Średnica rury, R_g – promień gięcia). W wyniku zastosowania takiej metodyki można przeprowadzić proces gięcia (o kącie do 180°) i otrzymać w obszarze gięcia owalizację i pocienienie ścianki znacznie mniejsze niż w otrzymywanych obecnie wyrobach. Obecnie stosowane metody gięcia oraz urządzenia gnące pozwalają osiągnąć minimalny promień gięcia nie mniejszy niż trzykrotność średnicy zewnętrznej rury.

Hipoteza badawcza zakładała, że istnieją efektywniejsze od dotychczas znanych sposoby gięcia rur. Sposoby te nie są oparte na kołowych profilach gnących, lecz mogą uwzględniać inne niezbadane dotychczas profile form kształtujących. Stosowane w praktyce kołowe wykroje zawodzą w ten sposób, że, nie dają efektów na małych promieniach, nie sterują (nie umożliwiają właściwego przepływu materiału w strefie gięcia). Analiza literatury wykazała, iż nie istnieją obecnie żadne opracowania teoretyczne, analizy numeryczne oraz weryfikacje doświadczalne dotyczące procesów beztrzpieniowego gięcia rur na małych promieniach tj. dla $1.5D \leq R \geq 2.5D$, gdzie: (R – promień gięcia, D – średnica zewnętrzna rury) do kąta 180°. Autorzy pracy w podejściu do modelowania numerycznego zagadnienia z uwagi na brak opracowań w tym zakresie (gięcie małych promieni) kierowali się własnym doświadczeniem w tej dziedzinie i dokonali wszelkich starań, aby założony model numeryczny jak najbardziej uprawdopodobnić z rzeczywistym procesem. Wspomagali się jedynie ogólną wiedzą zgromadzoną w literaturze nt. modelowania numerycznego. Reasumując celem publikacji jest wykazanie, iż zmiana kształtu wybrania wzornika w kierunku kształtu zbliżonego do elipsy skutkuje zmianą charakterystyki płynięcia (przemieszczania się) metalu po obwodzie rury i zmianą charakterystyki naprężeń a w konsekwencji zmianę kształtu przekroju rury w strefie gięcia.

Prezentowane w pracy badania polegają na poszukiwaniu właściwego przepływu materiału w przekroju rury w strefie gięcia poprzez ustalenie najbardziej efektywnego kształtu wybrania w wykroju oraz kształtowaniu powierzchni tarcia, przez co zostaną wyeliminowane: nadmierna owalizacja i pocienienie ścianki górnej. Przewidywanym efektem zastosowania tej technologii gięcia będzie zwiększenie wydajności przepływu w instalacjach energetycznych, co ma związek bezpośredni związek ze spadkiem emisji CO do atmosfery w wyniku mniejszego zużycia energii. Ponadto w pracy przedstawiono koncepcje narzędzi do doświadczalnej weryfikacji procesu gięcia rur.

* CZESTOCHOWA UNIVERSITY OF TECHNOLOGY, FACULTY OF PRODUCTION ENGINEERING AND MATERIALS TECHNOLOGY. 42-200 CZESTOCHOWA, 19 ARMII KRAJOWEJ AV., POLAND

** CZESTOCHOWA UNIVERSITY OF TECHNOLOGY, FACULTY OF MECHANICAL ENGINEERING AND COMPUTER SINCE

Corresponding authors: jm@wip.pcz.pl

1. Introduction

The application of tube bending processes in industrial practice is often a necessity due to the need for forming of different types of transmission systems and support structures, as well as out of consideration for the aesthetic of appearance [1,2].

Bending of tubes is an elasto-plastic forming process, which involves the simultaneous formation of both compressive and tensile stresses in the tube. The acting bending moment produces longitudinal tensile stresses and circumferential compressive stresses in the outer part of the bending zone. In the inner part of the bending zone, the moment causes longitudinal and circumferential compressive stresses. Such a distribution of stresses results in a thinning of the tensioned wall part and a thickening of the lower wall part [1,2,3].

Tube bending is accompanied by various phenomena characteristic of this process, which can be categorized into two groups:

a) change in the shape of the tube cross-section (tube cross-section ovalization), change in the tube wall thickness, elastic primary deformation, displacement of the neutral layer, changes in the strength properties, and
b) change in the mechanical properties.

All of the above-mentioned phenomena are adverse to the tube bending process, with the number of their occurrences being dependent on the bending method used.

Generally, tube bending methods are divided into:

- mandrel methods, and
- mandrelless methods [4].

Mandrel bending is applied to thin-walled tubes, when bending on small radii and with large angles, where there is additionally a possibility of bringing the mandrel in to the bending zone. The mandrel prevents the wall of the tube being bent from collapsing inside the tube. It also prevents the ovalization and flattening of the cross-section. The contour, on which tube is bent, is normally a semicircle with a radius equal to the radius of the bent tube [5,6,7].

In the mandrelless bending method, tube can be pressed on to the die with a roller or other elements, and the die shape does need to be a semicircle. Mandrelless bending methods are used for bending thick-walled tubes. Parameters that necessitate the use of a specific method include the relative wall thickness and the bending radius and angle. The degree of difficulty in conducting a bending operation is the higher, the larger the bending radius and the relative wall thickness are. As bent tubes are normally constructional elements, mechanical and aesthetic requirements are imposed on them. Not without importance are also the dimensions and shape of the inner cross-section, popularly called the clearance, which determine the efficiency of liquid flow within the tube. An example can be heat exchangers, transmission systems and hydraulic systems in machinery and means of transport (aircraft).

As the basic criteria for the assessment of bent tube, the following are assumed in practice:

- ovalization of the tube cross-section in the largest flattening location,
- wall thinning, and
- folding of bent tube length.

The ovalization is defined by the formula [4]

$$e = \frac{D_{\max} - D_{\min}}{D_{\max} + D_{\min}} \cdot 100\% \tag{1}$$

where: D_{max} - the greatest tube diameter in the largest flattening location

D_{min} - the smallest tube diameter in the same location.

Ovalization should not exceed:
- 12% for $R \leq 2D_z$
- 8% for $R \geq 2D_z$

where: D_z – nominal tube outer diameter
R – bending radius.

The tube thickness after thinning should not be less than 80% of the original thickness.

In order to take the control measurement of tube ovalization in the bent location, a control ball of a diameter of 0.86d for R≤3Dz and 0.9d for $R \geq 3D_z$ should be passed through the bent tube (where: d – tube inner diameter, R – bending radius, D_z – outer tube diameter).

Tube thinning s, or the relative thickness of the tube being bent (or the elbow formed), which is defined as the ratio of the wall thickness g to the outer diameter D_z of the bent tube (or the diameter of the finished elbow tube), is determined from formula [4,5]:

$$s = \frac{D_z}{g} \tag{2}$$

where: g – tube wall thickness
D_z – nominal tube outer diameter.

A schematic diagram of changes occurring during tube bending is shown in Fig. 1.

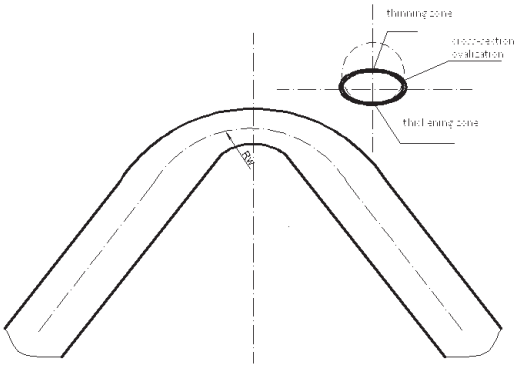

Fig. 1. Material thinning and ovalization in tube bending [6]

2. Assumptions and development of the design and impression of the die

The processes of small-radius ($R_g < 3D_z$) bending of tubes are normally effected using dies with a circular recess. For

bending long tubes (up to 12 m) meeting the criteria outlined above, press bending technology is used. A schematic diagram of the commonly used bending process is shown in Fig. 2. Figure 3 shows a classic die with a circular impression.

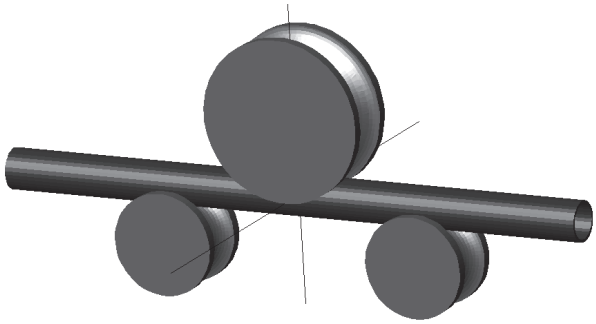

Fig. 2. Schematic diagram of the press tube bending process. 1. impression roller, 2. tube, 3,4 bending rollers

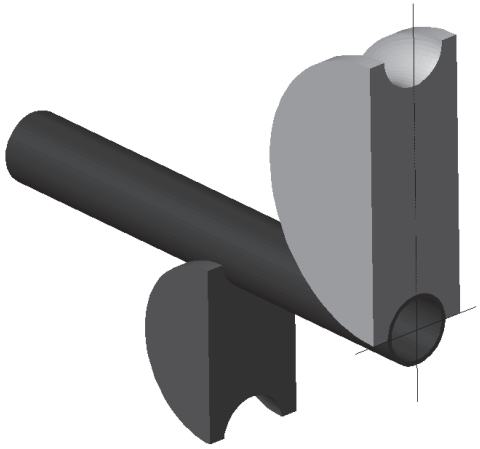

Fig. 3. Example of a tube bending die with a circular impression. 1. die, 2. tube, 3. roller

A major limitation when using the bending schematic as shown in Fig. 2 is to obtain a bending angle in the range of 160° ÷ 180° for a roller impression (recess) of a shape corresponding to the tube contour. Thus bent tubes undergo flattening, while the elbow inner wall collapses (Fig. 1). Figure 4 illustrates the design of the die and the tube bending die recess shape used.

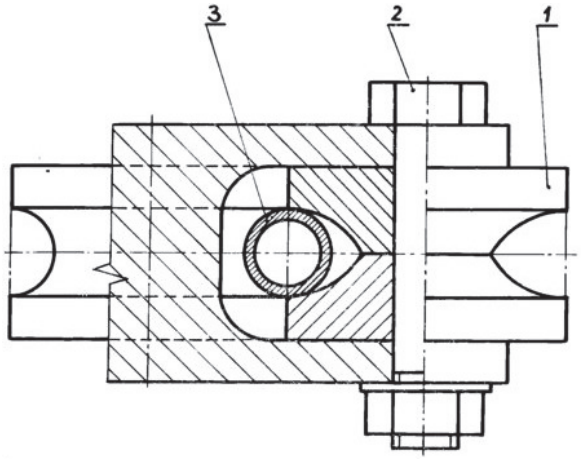

Fig. 4. The developed small-radius tube bending die and the die recess contour – the description in the text

The die is composed of at least two parts joined together in a detachable manner. The die parting plane is parallel to plane of symmetry of the recess. The recess contour radius is greater than half of the tube diameter. Die 1 has the form of a roller with a recess on the roller side surface. The die is divided into two parts joined together detachably with screw 2. The partition runs in the recess symmetry plane. The recess contour radius in each die part is equal to the diameter of the bent tube 3. Tube with an outer diameter of 25 mm and a wall thickness of 2.6 mm was subjected to bending. The bending was done up to a bending angle of 180°. The ovalization should not exceed then 2%.

The die impression was developed based on an elliptical design, as shown in Fig. 5.

During the analysis and discussion of the issues of small-radius mandrelless tube bending, it was quite accidentally discovered that the change to the recess in the die caused changes in ovalization of the tube cross-section in the bending zone. It was proposed then that the approach to the study of the problem from the side of examining the effect of the die recess shape on the cross-section ovalization in the bending zone would be the main course of the research. By the trial and error method, through numerical modelling, the direction in which to shape the die recess was determined numerically, and tests showed clearly that an elliptical or similar recess shape should be used, Fig. 5. By contrast, the use of a parabolic Fig. 6b recess shape had the opposite result, i.e. an increase in the wall collapse above the neutral axis.

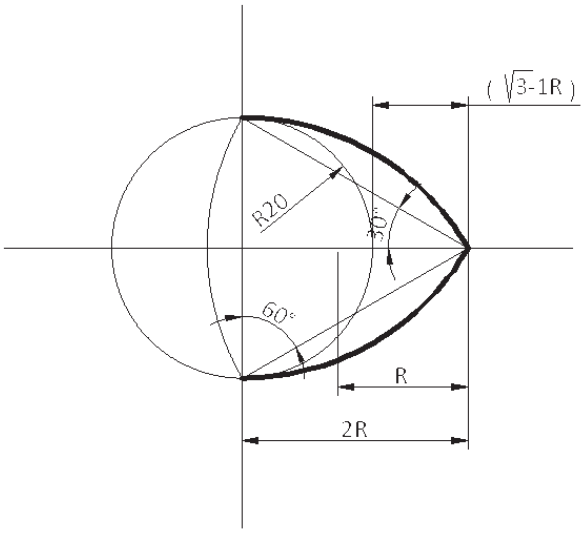

Fig. 5. The developed geometry of the die recess.

The developed recess contour is formed by the curvilinear sections and assumes the movement of the compressed tube regions toward the centre of the curvature (inside the recess).

3. Numerical modelling of the bending process

Preliminary model studies were performed with the FEM method using the commercial software program Forge®3D. For the FEM modelling, the developed impression of the elliptical design (Fig. 5) was used, while allowing for the contact of the

tube with the recess surface over a length of 2.5 and 5 mm, respectively. The case of bending using a conventional circular impression and a triangular die was also subjected to numerical examination. The paper reports results for extreme bending conditions, i.e. for the smallest bending radius corresponding to $1.5D_z$, where D_z is the tube outer diameter. Figure 6 shows models of the impressions (recesses) of the dies used in numerical calculations.

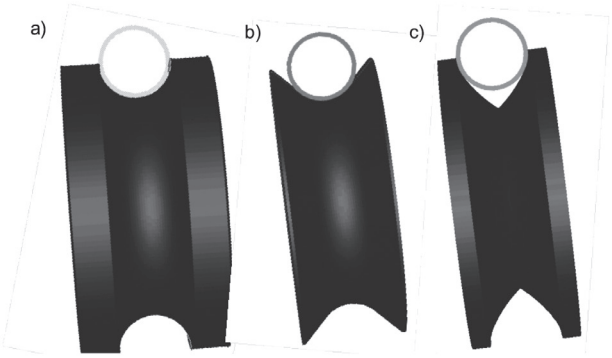

Fig. 6. Modelled bending die impressions: a) circular (conventional) impression, b) triangle impression, c) elliptical impression.

During numerical modelling, a constant bending velocity of V_g=10 mm/s was used for all impressions, while the bending angle a was 180°. The feedstock was tube with an outer diameter of D_z=25 mm and a wall thickness of g = 2.6 mm. The model material was the copper alloy E–Cu57 according to DIN, used in hydraulic systems [6].

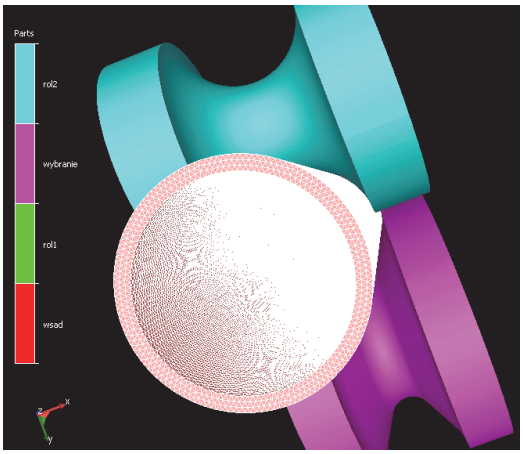

Fig. 7. The FEM elements in cross – section of pipe

The rheological properties of the model material, i.e. hydraulic copper E–Cu57 to DIN were taken from the database of the numerical software program Forge®3D 2011. For solving the problems of three-dimensional plastic metal flow during tube bending in die recesses, a mathematical model was selected, in which the mechanical state of the material being deformed was described using the Norton-Hoff (3) law [8, 9, 10, 11], which can be expressed with the equation below:

$$S_{ij} = 2K(T,\dot{\varepsilon},\varepsilon)(\sqrt{3}\,\varepsilon)^{m-1}\,\dot{\varepsilon}_{ij} \qquad (3)$$

where: Sij – stress tensor deviator, [11,12]

$\dot{\varepsilon}$ – strain rate intensity,

$\dot{\varepsilon}_i$ – strain rate tensor,

ε – strain intensity,

T – temperature,

K – consistence dependent on the yield stress, sp,

m – coefficient characterizing hot metal deformation ($0 < m < 1$).

The Coulomb friction model was used for the computation. The tube wall thickness was g=2.6mm; therefore, 3 finite elements were used, which allowed accurate stress and strain computation results to be obtained, especially in the tube bending zone (Fig. 7.). In view of the fact that this number of elements ensures a reasonable computation duration and that process optimization with a larger number of parameters (speed, friction, recess shape) is planned in future, no greater number than 3 was used for grid elements in the tube cross-section. Also, no model optimization procedure was conducted.

The developed concept of bending in the new impression assumes a minimization of the cross-sectional ovalization and the wall collapse due to the formation of the thinning and thickening zones (Fig. 1). Figure 8 shows, on the example of stress intensity distribution, a cross-sectional view of successive phases of bending tubes up to an angle of 180°, while using a bending radius of R_g<$1.5D_z$ in the bending zone for, respectively: a) a circular impression (conventional), b) a triangular impression, and c) an elliptical impression.

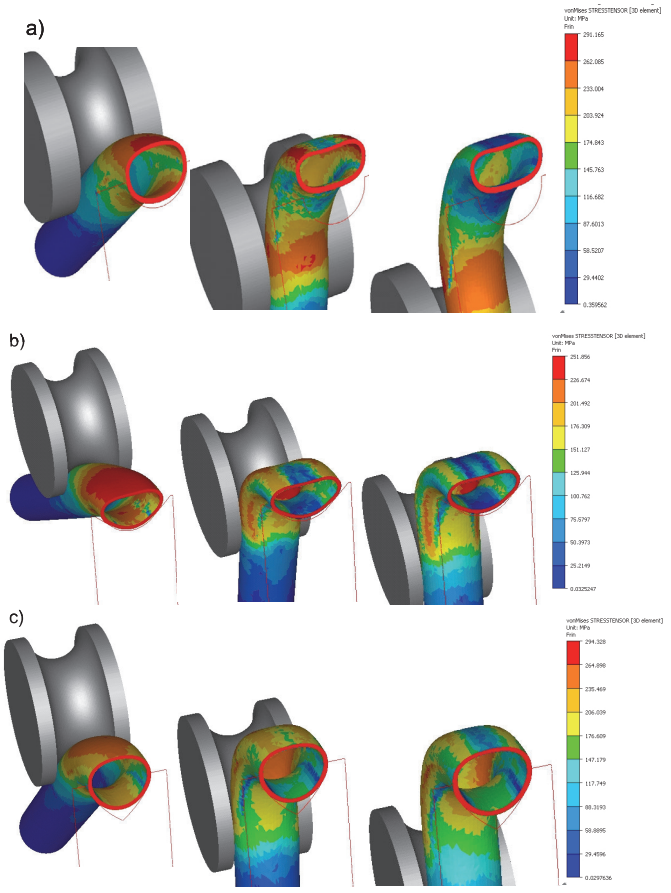

Fig. 8. Modelling of the tube bending processes for a bending radius of R_g=$1.5D_z$; a) the circular impression, b) the triangular impression, c) the elliptical impression.

The aim of the numerical modelling was to use die impressions other than circular during tube bending. As the first impression variant, a circular impression was used to assess the degree of ovalization. As suggested by the numerical computation results represented in Fig. 8a, the ovalization phenomenon occurs to a large extent in the circular impression, with an accompanying excessive tube bend. This is shown in detail in Fig. 9.

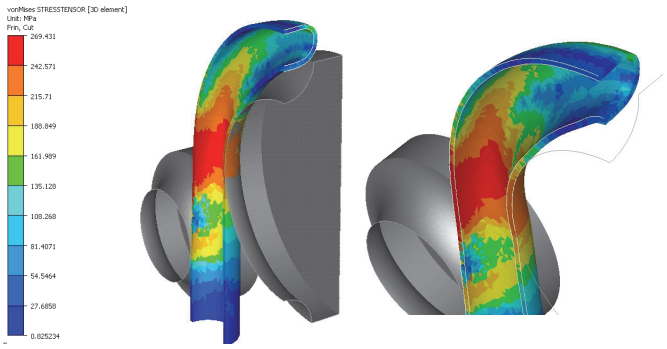

Fig. 9. Longitudinal section with a cross-section ovalization and a bend shown – a circular impression

The visible bend provides a confirmation of the theoretical assumptions made in the literature [4].

The use of the triangular impression has increased the degree of ovalization,

however, due to a reduction of compressive stresses, no distortion and collapse of the lower wall part have resulted. This is illustrated in Fig. 10.

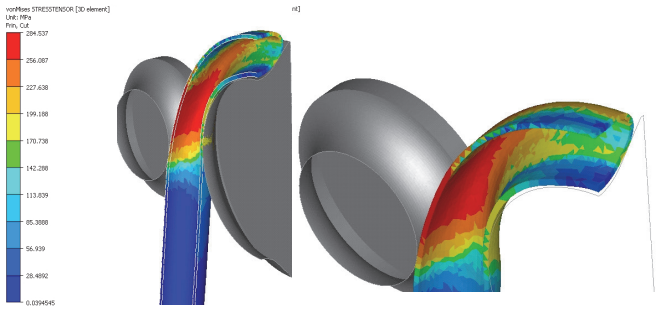

Fig. 10. Longitudinal section with a cross-section ovalization shown and without a visible bend – a triangular impression

The employed triangular impression has reduced the longitudinal and circumferential compressive stresses, which has resulted in a reduction of the tube wall flattening in the lower zone (below the neutral layer) and a break in the inner part of the bend due to an excessive shortening of metal fibres.

In the new proposed elliptical impression, the ovalization phenomenon is much smaller, and no excessive fibre shortening neither a break of the inner bend part occurs nor. (Fig. 11). Stress magnitudes on the section before the bend as compared to the circular impression are smaller by approx. 30 MPa.

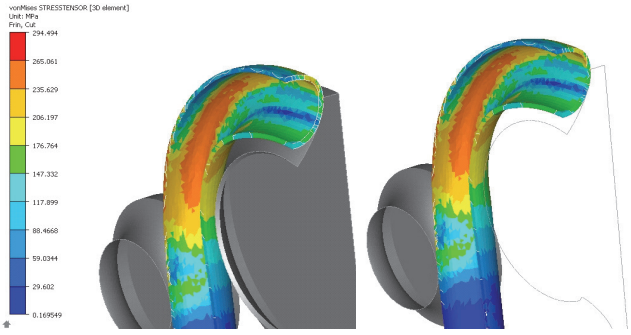

Fig. 11. Longitudinal section with a much smaller cross-section ovalization shown, without a visible bend – an elliptical impression

Figures 12, 13 and 14 represent strain intensity distributions for an elliptical, a circular and a triangular die impression, respectively. As shown by the presented numerical computations, the magnitudes of strain intensities in the bend zone are the smallest for the elliptical impression die variant.

During the process of tube bending in the elliptical impression, the strain intensity at the time of tube elbow forming (wrapping around the die) is approx. 0.14÷0.21 on the walls above and below the neutral axis. For the circular impression, the strain intensity in the regions of the greatest deformations (above and below the neutral axis) is considerably greater, being in the range of 0.28÷0.40. With the use of the triangular impression, intermediate strain intensity values at a level of 0.19÷0.25 were found to occur.

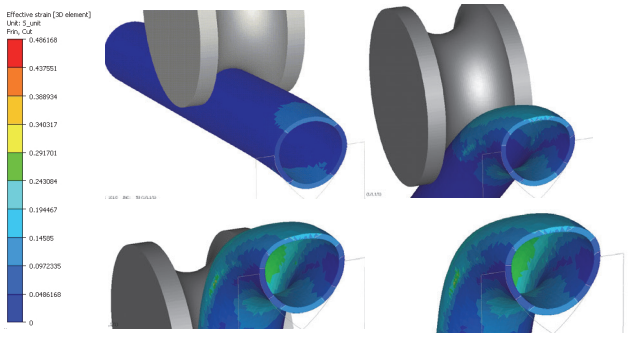

Fig. 12. Strain intensity distributions – the elliptical impression

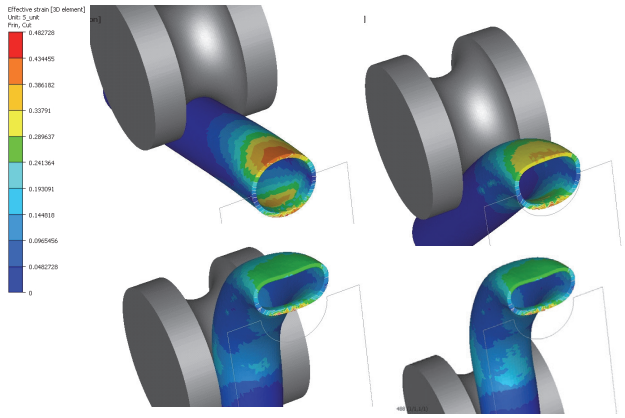

Fig. 13. Strain intensity distributions – the circular impression

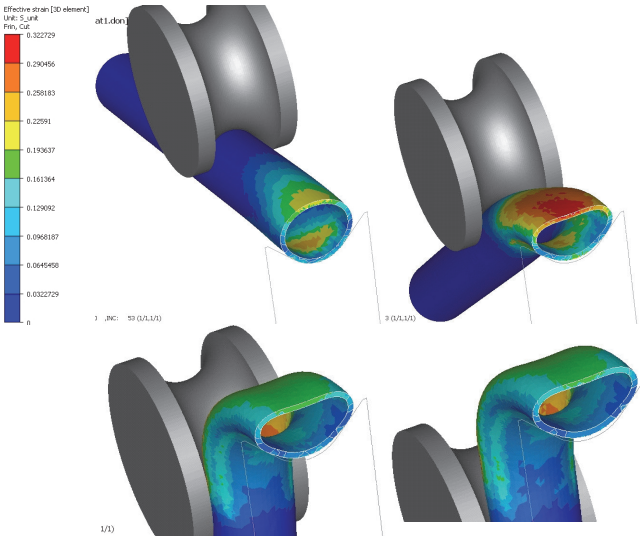

Fig. 14. Strain intensity distributions – the triangular impression

The obtained results represented in Fig. 8 and in Figs. 12, 13 and 14 enable one to conclude that using the elliptical impression (composed of curvilinear sections) does not result in the formation of compressive stresses below the neutral axis in the tube bend part with a magnitude causing an excessive metal fibre shortening and a flattening or collapse of the wall. Therefore, the cross-section ovalization is much smaller than for the circular and triangular impression die variants. The elliptical recess contour allows the compressed tube regions to move towards the curvature centre (into the die recess/ impression).

4. The concept of a physical test tool

The idea of small-radius tube bending up to an angle of a= 180° embraces also the capability to carry out the process on hydraulic and mechanical presses. In addition, the concept assumes also bending tubes of lengths up to 12 m. Figure 15 illustrates schematically a tool for carrying out physical testing.

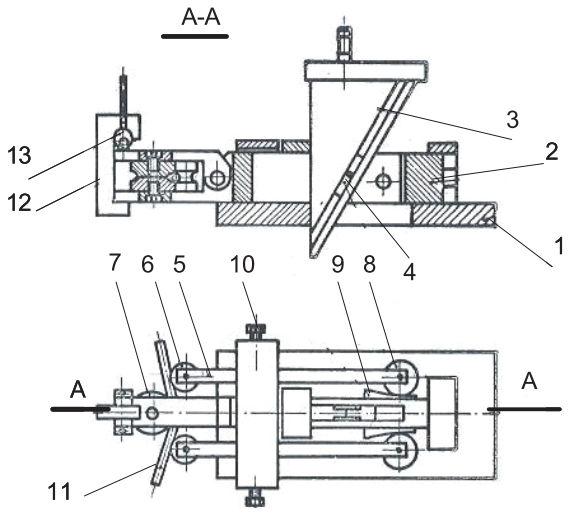

Fig. 15. Schematic diagram of the tool. 1 – plate, 2 – slide, 3 – taper key, 4 – inserts, 5 – levers, 6 – bending rollers, 7 – die, 8 – rollers, 9 – cams, 10 – screws, 11 – tube, 12 – clamp, 13 – eccentric

The tool has plate 1, on which slide 2 is mounted, which is driven by taper key 3. The taper key has grooves milled in it, in which inserts 4 are seated. They are connected with the main slide. The inserts allow the slide to be retracted after completion of the bending operation. There are levers 5 on either side of slide 2, which enable tube 11 to be bent down to eliminate the springing angle. The levers are ended with rollers on both sides. Rollers 8 roll along the cams and cause the bent tube ends to be bent down by pressing on with rollers 6. Tube 11 is being bent on split die 7 with an appropriately selected recess contour. To change the bending radius, die 7 is replaced and the position of lever 5 is adjusted using screws 10. Also, rollers 8 can be replaced.

Bending of tube 11 is effected by placing it between rollers 6 and die 7. Then, the die is closed up with clamp 12. Slide 2 driven by taper key 3 moves and draws the tube between rollers 6. After attaining the bending angle, the retracting taper key causes the reverse motion of the slide. The bending plane is horizontal.

5. Summary

The numerical studies have shown that mandrelless small-radius tube bending (with $1.5D_r<R_g<2.5D_z$, where D_z – tube diameter, R_g – bending radius) using impressions with a circular and a triangular shape is ineffective, primarily because of the cross-section ovalization and the product bend due to considerable plastic strains in the outer and the inner bend parts. The proposed new die impression/recess contour formed from curvilinear sections delineating an ellipse provided the capability to move the compressed tube regions towards the centre of the curvature. This resulted in a reduction of the collapse of the tube wall of the outer bend part, and thereby a lesser ovalization. In addition, by moving upwards along the tube perimeter, the material did not cause a tube bend, as was the case when bending using the circular impression die. The compressive stresses in the inner bend part assumed the smallest magnitude for the elliptical impression die. Undoubtedly, also the friction at the tube–die interface played an important role, which hampered such a flow of metal, especially in the circular impression variant, where the tube was totally clamped.

The aim of presenting this approach to the problem to the extent, as covered in the paper, was to show the scientific environment that the authors of the paper had an original, developed by them concept for effective small-radius tube bending. As there are no studies nor research directions on this subject (mandrelless small-radius bending up to an angle of 1800) known to the authors, they decided initially to develop the theoretical basis of the process by using the trial and error method and determine the die shape, which would not cause the wall collapse and the occurrence of excessive ovalization. Such a recess has, as a consequence, the shape of an ellipse, as shown in Fig. 5 and 6. The next stage of the research will be to optimize both the recess shape and the tube and die contact surface, and to examine the effect of the change in bending speed and friction. After obtaining the preliminary results presented in this paper, regarded by the authors as promising, it will be crucial in

subsequent research to obtain the smallest possible degree of tube ovalization, i.e. a value contained within the limits specified by the standard. The last stage of the research will be experimental verification according to the tool design as in Fig. 15.

REFERENCES

[1] S. Erbel, K. Kuczyński, Z. Marciniak, Obróbka plastyczna, Warszawa 1981.
[2] F. Stachowicz, J. Mater Process Tech. 100, 236 – 240 (2000)
[3] J. Kazanecki, Wytwarzanie rur bez szwu. Kraków 2003.
[4] W.P. Romanowski, Poradnik Obróbka Plastyczna na zimno, Warszawa, 1976.
[5] J. Pacanowski, Z Kosowicz, Rudy i Metale Nieżelazne. R41: nr 10, 419 – 423 (1996).
[6] W. Kubiński, M. Kuczera, Obróbka Plastyczna Metali 5, 5 -24 (2003).
[7] M. Zahn. J Mater Process Tech. **127**, 401 – 408 (2002).
[8] A. Stefanik , H. Dyja, S. Mróz, Arch. Metall. Mater. **56**, 2 (2011).
[9] M. Kopernik, M. Pietrzyk, Arch. Metall. Mater. **52**, 2 (2007).
[10] J.L. Chenot, L. Fourment, T. Coupez, R. Ducloux, E. Wey, Forging and Related Technology. Birminghams, 113, (1998).
[11] Hoff N.J, Quart, Appl. Mech. **2**, 49 (1954).
[12] Norton F.H, Creep of Steel at High Temperature. McGraw Hill, New York 1929.

Received: 15 September 2014.